Tissue Characterization of Coronary Plaques
—— Comparison of Integrated Backscatter Intravascular Ultrasound With Virtual Histology Intravascular Ultrasound ——

Munenori Okubo, MD**; Masanori Kawasaki, MD**; Yoshiyuki Ishihara, MD; Urara Takeyama, MD; Shinji Yasuda, MD; Tomoki Kubota, MD; Shinichiro Tanaka, MD; Takahiko Yamaki, MD; Shinsuke Ojio, MD; Kazuhiko Nishigaki, MD; Genzou Takemura, MD; Masanao Saio, MD*; Tsuyoshi Takami, MD*; Hisayoshi Fujiwara, MD; Shinya Minatoguchi, MD

Background Integrated backscatter (IB) intravascular ultrasound (IVUS) and IVUS Virtual Histology (VH) have been developed for tissue characterization, but have never been compared directly. The purpose of this study was to compare the overall agreement between IB-IVUS and IVUS-VH in the tissue characterization of plaques from the same coronary arterial cross-section.

Methods and Results Images were acquired from 46 coronary arteries from 25 cadavers. Of a total of 392 histology/IVUS image pairs, 152 pairs were diagnosed as Stary's type Ⅲ, IV, Va, Vb and Vc, and compared for IB-IVUS, IVUS-VH and histology. In the qualitative comparison, the overall agreement between histological and IB-IVUS diagnoses was higher (κ=0.81, 95% confidence interval (CI): 0.74–0.89) than that of the IVUS-VH diagnoses (κ=0.66, 95%CI: 0.56–0.75). The % fibrosis area determined by IB-IVUS was significantly correlated with the relative area of fibrosis based on histology (r=0.67, p<0.001). In the quantitative comparison, the overall agreement between the histological and IB-IVUS diagnoses was higher (κ=0.83, 95% CI: 0.75–0.91) than that of the IVUS-VH diagnoses (κ=0.73, 95% CI: 0.63–0.83).

Conclusion Based on histology as the gold standard, IB-IVUS provided higher diagnostic accuracy than IVUS-VH for tissue characterization of coronary plaques.

Key Words: Imaging; Plaque; Tissue; Ultrasonics

Pathologic and angioscopic studies have demonstrated that plaque rupture into the vessel lumen may lead to the formation of thrombus and acute coronary syndrome (ACS)[1,2] Evaluation of the tissue characteristics of coronary plaque is important to understand the process of ACS and prevent it, because the stability of atherosclerotic plaque is related to histological composition. Accurate in vivo identification of the tissue characteristics of coronary plaque may allow the identification of vulnerable plaques before the development of ACS.

Intravascular ultrasound (IVUS) provides a comprehensive assessment of atherosclerotic plaques in vivo;[3] many techniques for tissue characterization of plaque composition have been developed.[4–6] We reported that ultrasound integrated backscatter (IB) values reflect the tissue characteristics of human coronary arterial plaques,[7–9] and it has also been reported that IVUS Virtual Histology (VH), using autoregressive analysis of radiofrequency (RF) signals, allows plaque characterization of coronary arteries.[10,11] Because these 2 systems use different algorithms, it is possible that there may be differences in their ability to identify the tissue characteristics of coronary plaque, so the purpose of the present study was to compare the overall agreement between IVUS images and histology in the tissue characterization of plaques from the same coronary arterial cross-section and to evaluate the advantages and limitations of each of these modalities, using histological images as the gold standard.

Methods

Specimens

We examined 392 cross-sections of 46 diseased coronary arteries from 25 cadavers (18 had symptomatic cardiovascular disease (72%)). The coronary arteries were dissected within 24 h of death and immediately fixed with 10% buffered formalin solution and stored for more than 24 h. The experimental protocol was approved by the institutional ethics committee and in all cases informed consent was given by the relatives of the patients for the ex vivo study.

(Received November 12, 2007; revised manuscript received May 7, 2008; accepted May 26, 2008; released online August 28, 2008)
*Regeneration & Advanced Medical Science, *Department of Immunopathology, Gifu University Graduate School of Medicine, Gifu, Japan*
We have no financial or other relations that could lead to a conflict of interest.
**The first two authors contributed equally to this work.
Mailing address: Masanori Kawasaki, MD, Regeneration & Advanced Medical Science, Gifu University Graduate School of Medicine, 1-1 Yanagido, Gifu 501-1194, Japan. E-mail: masanori@ya2.so-net.ne.jp

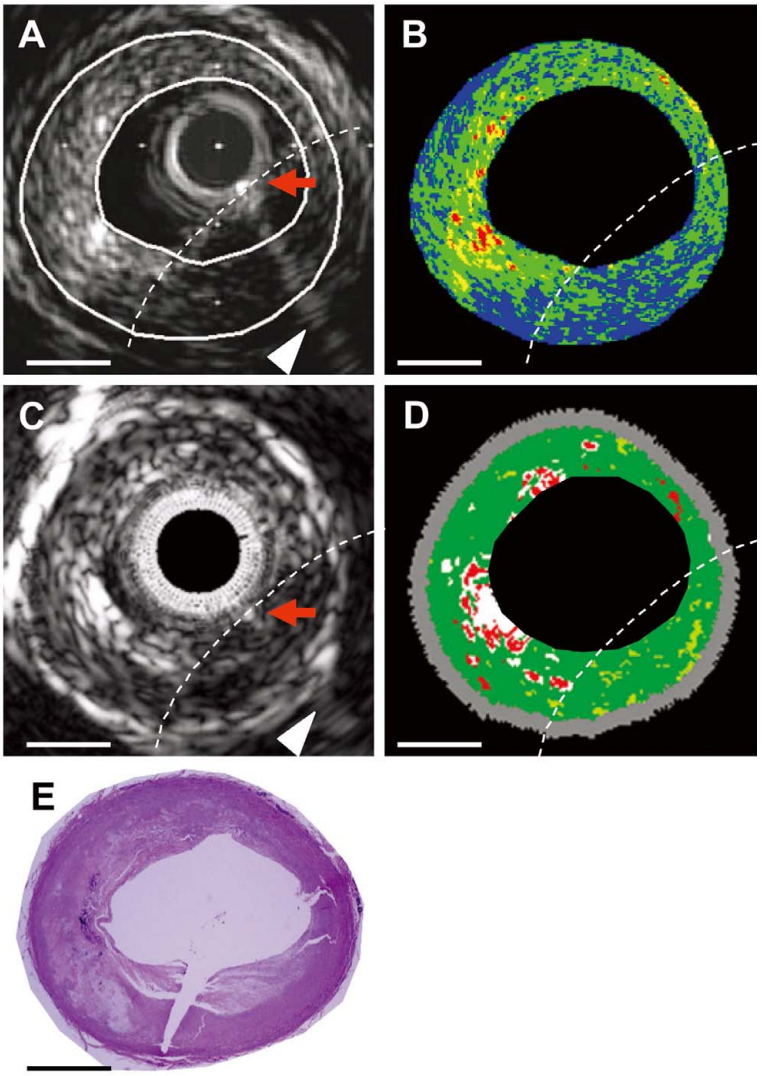

Fig 1. Corresponding cross-sections of each intravascular ultrasound (IVUS) image and its histology (broken line indicates the track of a surgical needle). Bar=1 mm. (A) Conventional IVUS image containing a surgical needle (arrow) that was acquired using a 40-MHz mechanical rotating catheter. Arrowhead, reverberation phenomenon of the surgical needle. (B) Integrated backscatter-IVUS image. (C) Conventional IVUS image containing a surgical needle (arrow) that was acquired using a 20 MHz phased-array catheter. Arrowhead=reverberation phenomenon of the surgical needle. (D) IVUS-Virtual Histology image. (E) Histological image. We identified the histological cross-section in which this specimen was torn at the site of the surgical needle as the cross-section corresponding to IVUS imaging.

IB-IVUS Data Acquisition

To obtain IB-IVUS images, the system (IB-IVUS, YD Co, Ltd, Nara, Japan) was connected to an imaging system (Clear View, Boston Scientific, Natick, MA, USA) with RF output, signal trigger output and video image output to obtain the RF signal. Ultrasound backscattered signals were acquired using a 40-MHz mechanically-rotating IVUS catheter (Atlantis, Boston Scientific), digitized and subjected to spectral analysis. The IB values for each tissue component were expressed in decibels (dB) and calculated using a fast-Fourier transform of the frequency component of the backscattered signal from a small volume of tissue. Conventional IVUS images and IB-IVUS color-coded maps were displayed side-by-side on a monitor. We excluded the vessel lumen and area outside of the internal elastic membrane from the IB-IVUS color-coded maps by tracing the vessel lumen and internal elastic membrane on the conventional IVUS images. In the IB-IVUS images, color-coded maps have 4 major components: fibrous (green), dense fibrosis (yellow), lipid pool (blue), and calcification (red). These technical settings were described in a previous report.[12]

Correlation Between IB-IVUS and Histology Images

After formalin fixation, the arterial segments were subjected to IVUS imaging in phosphate-buffered saline at a temperature of 37°C. IVUS imaging was performed within 48 h of death. Several studies have documented that formalin fixation does not significantly affect the quantitative echo character of plaque tissue from human aortic walls.[13,14] In addition, we previously confirmed that the IB values of arteries with a constant pressure before fixation were similar to those of non-pressured arteries after fixation at the same site in a comparison of 50 cross-sections of 10 coronary arteries obtained at autopsy from 5 cadavers.[12] In that study, the Bland-Altman plot showed that the differences between the IB values of pressured arteries before fixation and non-pressured arteries after fixation were within 2 standard deviations of the mean difference; there was also an excellent correlation between the 2 methods ($r=0.99$, $p<0.001$). Ultrasound backscatter power was proportional to the difference of acoustic characteristic impedance that was determined by the density of tissue multiplied by the speed of sound. There seems to be no significant influence of formalin fixation on acoustic characteristic impedance, whereas formalin fixation decreases the distensibility significantly in non-calcified arteries.[15]

IVUS-VH Image Acquisition and Comparison With IB-IVUS Images

IVUS-VH (Virtual Histology Version 1.4, Volcano Corp,

San Diego, CA, USA) images were acquired by an IVUS-VH console with a 20-MHz phased-array catheter and stored on CD-ROM for offline analysis. To clarify the rotational and cross-sectional position of the included segment, multiple surgical needles were carefully inserted into the coronary arteries before IB-IVUS and IVUS-VH imaging to serve as reference points for comparison of the 2 imaging modalities (Fig 1). This method was successfully used in previous comparative studies of histology and IVUS images![10,12,16] Next, the catheter was advanced into the coronary arteries and pulled back at 0.5 mm/s by activating an auto-pullback device. The ECG-triggered acquisition system for the IVUS-VH images was disabled and a time-dependent (1 image/s) trigger was added to obtain the IVUS-VH images. IB-IVUS images were also acquired at an interval of 1/s using the auto-pullback device. Cross-sectional images from sites containing surgical needles and from sites within 1 mm of the needles were obtained to ensure that IB-IVUS and IVUS-VH images were compared at exactly the same site. After the images were acquired, the sites were sutured with suture material attached to the needles to serve as a reference point when comparing the IVUS images with histology. Tissue maps of IVUS-VH have 4 major components: fibrous (green), fibro-fatty (light-green), necrotic core (red), and dense calcification (white).

Histological Analysis

Ring-like sections of arteries obtained at the same level as the imaging study were decalcified for 5 h, embedded in paraffin and cut perpendicular to the longitudinal axis of the artery into 2-μm sections. These were stained with hematoxylin-eosin, elastica van Gieson and Masson's trichrome. Of a total of 392 histology/IVUS image pairs, 152 pairs that were diagnosed as Stary's type Ⅲ, Ⅳ, Va, Vb and Vc according to consensus of 2 pathologists who were unaware of the IVUS images, were randomly selected![17] The longitudinal thickness of the ultrasound beam of the IVUS catheter (Atlantis, Boston Scientific) was more than 200μm, whereas the thickness of the histological cross-sections was 2μm. Therefore, we evaluated multiple histological cross-sections to obtain a histological diagnosis. The cross-sections in which the histological diagnosis was different within 200μm were excluded from the comparison (2 cross-sections). As described in the American Heart Association (AHA) classification[17] and modified AHA classification![18] type Ⅲ was defined as a pathological intimal thickening with a poorly formed fibrous cap, but without a necrotic core. Typically, such lesions show incompletely coalesced extracellular lipid. Type Ⅳ was defined as an atheroma with a well-formed fibrous cap overlying a confluent lipid core. Type V was defined as a lesion in which prominent new fibrous connective tissue had formed. When the new tissue was part of a lesion with a lipid core (type Ⅳ), this morphology was referred to as type Va lesion. A type V lesion in which the lipid core and other parts of the lesion were calcified was referred to as type Vb. When type V lesions show marked fibrosis and little lipid, they were referred to as type Vc. For quantitative comparison, coronary arterial cross-sections were also classified into 3 categories: fibrocalcific, fibrous and lipid-rich by the consensus of 2 pathologists who were unaware of the IVUS images

IVUS Image Classification

We performed "qualitative", "direct qualitative", "quantitative" and "direct quantitative" comparisons between IB-IVUS and IVUS-VH images. In the "qualitative" comparison, 150 IB-IVUS and IVUS-VH images were classified into Stary's type Ⅲ, Ⅳ, Va, Vb or Vc by the consensus of 2 IVUS readers who were unaware of the histological diagnoses. We performed a "direct qualitative" comparison by setting small (0.3×0.3 mm) regions-of-interest (ROIs) on the same sites in both the histological and IVUS images. Histological classification in the direct qualitative comparison was performed as per the previous reports![7,12,19] We then performed the "quantitative" comparison using the following definition. The 150 cross-sections were diagnosed as fibrocalcific, fibrous or lipid-rich by 2 IVUS readers who were unaware of the histological diagnoses. In the IB-IVUS images, the lesions that included calcification (red) and occupied >1% of the entire cross-section were diagnosed as fibrocalcific, regardless of the %lipid pool area, because we could recognize a calcified mass in the corresponding histological images when the red area was >1%. The lesions that included lipid pool (blue) and occupied >30%, and calcification (red) that occupied ≤1% of the entire cross-section and include a mass of lipid core were diagnosed as lipid-rich by IB-IVUS. Otherwise, the lesions were diagnosed as fibrous by IB-IVUS. In the IVUS-VH images, the lesions that included dense calcification (white) that occupied >5% of the entire cross-section were diagnosed as fibrocalcific, regardless of the %necrotic core area, because we could recognize a calcified mass in the corresponding histological images when the white area was >5%. The lesions that included a necrotic core (red) that occupied >10%, and dense calcification (white) that occupied ≤5% of the entire cross-section and included a mass of lipid core were diagnosed as lipid-rich, because the percentage of necrotic core (y) indicated by IVUS-VH was approximately one-third of the lipid pool (x) indicated by IB-IVUS ($y=0.34x$, $r=0.91$, $p<0.001$) at the same cross-section. Otherwise, the lesions were diagnosed as fibrous by IVUS-VH. This definition was determined using the remaining 240 of the 392 cross-sections.

Furthermore, we performed a "direct quantitative" comparison. Of the 150 histology/IVUS image pairs, we randomly selected 49 pairs in which the histological specimens were clearly stained with Masson's trichrome with sufficient resolution for quantification. These images were digitized and the areas that were stained blue were automatically selected by a multipurpose image processor (LUZEX F, Nireco Co, Tokyo, Japan). The relative fibrous area (fibrous area/plaque area) was then automatically calculated by the LUZEX F system. We were not able to quantitatively compare the lipid area and necrotic core area because the lipid area and/or necrotic core were partly corrupted and/or melted by the formalin fixation and microtome cuts necessary to the procedure. Of a total of 49 pairs, we selected 45 histology/IVUS image pairs for use in the "direct qualitative" comparison. In these 45 pairs, the shape of the cross-sections was not deformed by the process of formalin fixation, paraffin embedding and microtome cutting. When there were 2 diagnoses in the ROI, the diagnosis that occupied more than half of the area was selected. When there were more than 3 diagnoses in the ROI, the ROI was excluded from the comparison. A total of 141 ROIs were compared. When there was a small gap between the location of the ROIs placed on the IVUS images and histological images, referring to the vascular lumen and outside border, we adjusted the location of the ROIs.

Table 1 Qualitative and Quantitative Comparison of the IVUS and Histological Diagnoses

	Histological diagnosis								
	III	*IV*	*Va*	*Vb*	*Vc*	*LR*	*FI*	*FC*	*Total*
Qualitative comparison									
IB-IVUS diagnosis									
III (Preatheroma)	20	0	0	0	0				20
IV (Atheroma)	7	14	0	0	0				21
Va (Fibroatheroma)	0	0	21	8	4				33
Vb (Calcific lesion)	0	0	0	49	0				49
Vc (Fibrotic lesion)	0	0	0	0	15				15
Total	27	14	21	57	19				138
Cohen's κ=0.81 (95%CI: 0.74–0.89)									
IVUS-VH diagnosis									
III (Preatheroma)	14	0	0	0	0				14
IV (Atheroma)	11	12	0	0	0				23
Va (Fibroatheroma)	0	0	14	6	7				27
Vb (Calcific lesion)	0	1	1	50	3				55
Vc (Fibrotic lesion)	0	0	4	1	9				14
Total	25	13	19	57	19				133
Cohen's κ=0.66 (95%CI: 0.56–0.75)									
Quantitative comparison									
IB-IVUS diagnosis									
LR						60	8	4	72
FI						1	15	0	16
FC						1	0	49	50
Total						62	23	53	138
Cohen's κ=0.83 (95%CI: 0.75–0.91)									
IVUS-VH diagnosis									
LR						52	7	5	64
FI						4	12	1	17
FC						2	3	47	52
Total						58	22	53	133
Cohen's κ=0.73 (95%CI: 0.63–0.83)									

IVUS, intravascular ultrasound; LR, lipid-rich; FI, fibrous; FC, fibrocalcific; IB, integrated backscatter; CI, confidence interval; VH, virtual histology.

Table 2 Direct Qualitative Comparison of the IVUS and Histological Diagnoses

	Histological diagnosis								
	CL	*DF*	*FI*	*LP*	*DC*	*FI*	*FF*	*NC*	*Total*
IB-IVUS diagnosis									
CL	14	0	0	0					14
DF	2	3	0	0					5
FI	3	0	53	2					58
LP	2	0	8	54					64
Total	21	3	61	56					141
Cohen's κ=0.81 (95%CI: 0.72–0.89)									
IVUS-VH diagnosis									
DC					20	4	0	2	26
FI					1	25	11	16	53
FF					0	3	13	5	21
NC					0	28	1	12	41
Total					21	60	25	35	141
Cohen's κ=0.30 (95%CI: 0.14–0.41)									

CL, calcification; DF, dense FI; LP, lipid pool; DC, dense CL; FF, fibro-fatty; NC, necrotic core. Other abbreviations see in Table 1.

Reproducibility and Reliability of Data

We previously determined the inter-catheter variability of the cross-sectional areas in 18 recordings that were measured by 1 observer using 5 randomly selected IB-IVUS catheters[12] The inter-catheter variability of the lipid pool cross-sectional area and fibrous cross-sectional area was 6.1±6.9% and 4.1±3.2%, respectively. Likewise, we determined the intra-catheter variability of the cross-sectional areas in 18 images that were measured 3 times by 1 observer using 1 catheter selected at random. The intra-catheter variability of the lipid pool cross-sectional area and fibrous cross-sectional area was 2.6±1.7% and 0.73±0.38%, respectively. The interobserver agreement using IB-IVUS for characterization of plaque type was excellent (κ=0.84). A previous study reported that the limits of agreement for calcium, fibrous, fibrolipidic and necrotic core cross-sectional areas using IVUS-VH were 0.22, –0.25 mm^2; 1.02, –0.71 mm^2; 0.61, –0.65 mm^2; and 0.43, –0.38 mm^2, respectively.[20]

Statistical Analysis

The degree of agreement between the histological and

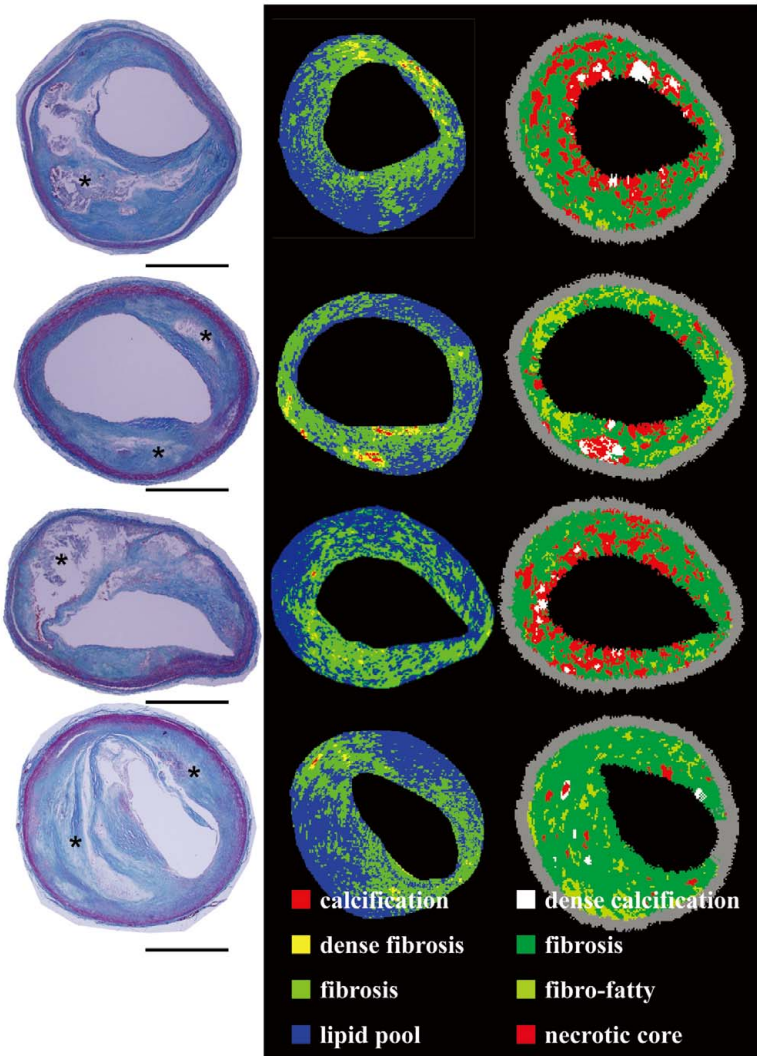

Fig 2. Representative lesion composed of a large lipid core with a thin fibrous cap. (Left) Histological image (Masson's trichrome staining). *Lipid pool. (Middle) Corresponding color-coded maps constructed by the integrated backscatter intravascular ultrasound system. (Right) Corresponding Virtual Histology intravascular ultrasound images.

IB-IVUS classifications, and the histological and IVUS-VH classifications was quantified by Cohen's κ test for concordance[21] A κ value of 0.61–0.80 indicates good agreement, and 0.81–1.0 indicates excellent agreement[22] The correlations between the relative fibrous area based on histology and the relative fibrous area based on IVUS were determined by linear regression analysis.

Results

Diagnostic Accuracy for Classifying Arterial Plaque

A total of 150 cross-sections were diagnosed as Stary's type Ⅲ, IV, Va, Vb and Vc by 2 IVUS readers who were unaware of the histological diagnoses. The 2 readers made identical diagnoses in 138 cross-sections by IB-IVUS and in 133 cross-sections by IVUS-VH. The interobserver agreement of IB-IVUS and IVUS-VH for tissue characterization of plaque type was excellent (Cohen's κ=0.90 and 0.85, respectively). Only the cross-sections in which the diagnoses were identical between 2 readers were used for comparison with histology, because we usually achieve a consensus of tissue characteristics from IB-IVUS or IVUS-VH images by more than 2 readers in the catheter laboratory in the clinical setting.

IB-IVUS and IVUS-VH Images Compared With Histology

In the qualitative comparison, the overall agreement between the histological and IB-IVUS diagnoses was higher (Cohen's κ=0.81, 95% confidence interval (CI): 0.74–0.89) than between the histological and IVUS-VH diagnoses (Cohen's κ=0.66, 95% CI: 0.56–0.75) (Table 1). In the quantitative comparison, the overall agreement between the histological and IB-IVUS diagnoses was higher (Cohen's κ=0.83, 95% CI: 0.75–0.91) than between the histological and IVUS-VH diagnoses (Cohen's κ=0.73, 95% CI: 0.63–0.83) (Table 1).

In the direct qualitative comparison, the overall agreement between the histological and IB-IVUS diagnoses was higher (Cohen's κ=0.81, 95% CI: 0.72–0.89) than between the histological and IVUS-VH diagnoses (Cohen's κ=0.30, 95% CI: 0.14–0.41) (Table 2). Representative IB-IVUS and IVUS-VH images are shown in Figs 2 and 3. Although the location of each tissue component depicted by IVUS-VH did not always accurately reflect the histological location, as shown in Figs 2 and 3, the overall agreement of IVUS-VH in the "quantitative" comparison (0.73) was better than that in the "qualitative" comparison (0.66), whereas the IB-IVUS values were similar (0.83 and 0.81).

In the direct quantitative comparison, the % fibrosis area determined by IB-IVUS significantly correlated with the re-

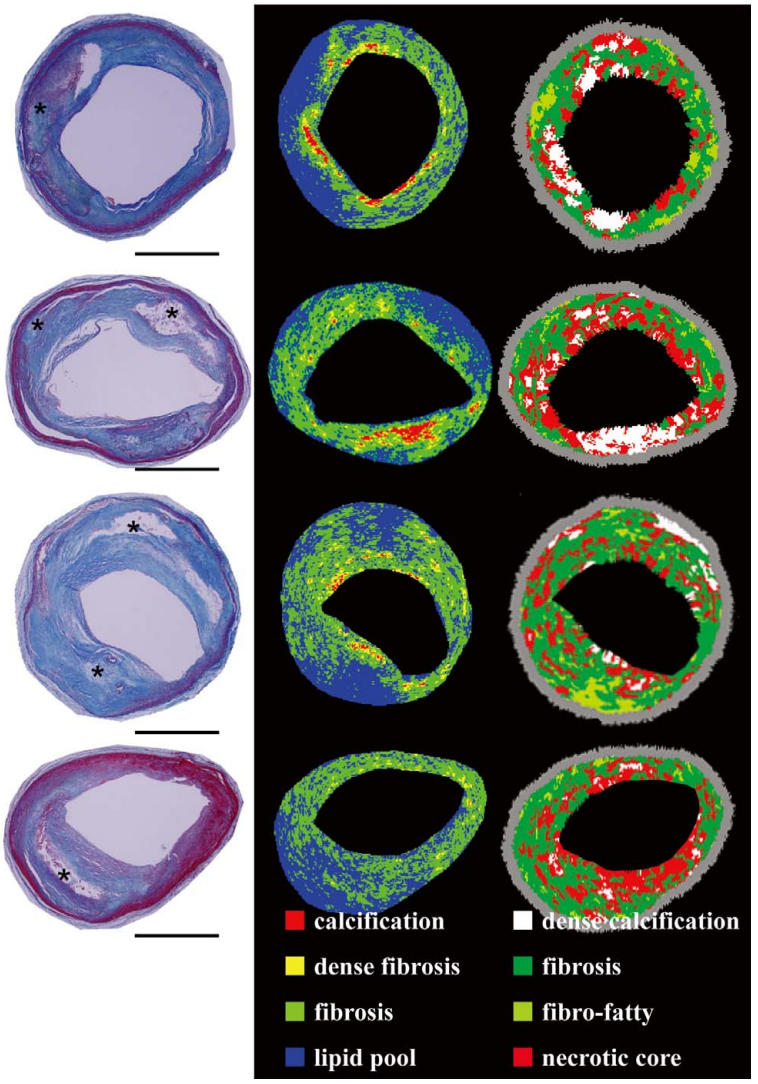

Fig 3. Representative lesion composed of a lipid core without a thin fibrous cap. (Left) Histological image (Masson's trichrome staining). *Lipid pool. (Middle) Corresponding color-coded maps constructed by the integrated backscatter intravascular ultrasound system. (Right) Corresponding Virtual Histology (VH) intravascular ultrasound (IVUS) images. IVUS-VH overestimated the necrotic core, which was located particularly close to the vessel lumen.

lative area of fibrosis based on histology (r=0.67, p<0.001), whereas the % fibrous area and % fibrous area+% fibro-fatty area determined by IVUS-VH did not correlate with the relative area of fibrosis based on histology (Figs 4,5).

Discussion

Diagnostic Accuracy of Tissue Characterization

There are a variety of catheter-based invasive methods of characterizing coronary plaque,[5–7] and of these optical coherence tomography (OCT) is a reliable and reproducible imaging modality for tissue characterization.[23] Atherosclerotic plaques can be discriminated ex vivo with a high degree of sensitivity (90–94%) and specificity (90–92%).[24] OCT imaging gives clear cross-sectional imaging in vivo, although it requires the removal of blood from the coronary arteries in the field of view to obtain high-quality images and the limited penetration depth precludes comprehensive evaluation of the entire vessel.[25] Recent IVUS studies characterized the tissue components of coronary plaque using an autoregressive classification scheme rather than depending on the classic Fourier method.[11,19] The analysis in those studies accounted for parameters such as the frequencies at maximum and minimum power and the slope of the regression line of ultrasound backscattered signals. The autoregressive tree classified fibrous, fibro-fatty, necrotic core and dense calcium with a high predictive accuracy of 87%, 87%, 88% and 97%, respectively. The analysis using IB values classified fibrous, lipid-rich, and fibrocalcific plaque components with a high predictive accuracy of 93%, 90% and 96%, respectively.[12] These values obtained using IB-IVUS were similar to those determined using the auto-regressive classification scheme. However, the present study demonstrated that the IB-IVUS system provides higher diagnostic accuracy than IVUS-VH for analysis of tissue characteristics of coronary plaque in a direct comparison using the same histological cross-sections.

Discrepancy Between IB-IVUS Findings and Histology

In the present study, a false-positive diagnosis by IB-IVUS of a lipid-rich lesion often contained histological evidence of much smaller lipid accumulation within a predominantly fibrous lesion. Lesions that included many small areas of lipid accumulation mixed with fibrosis were diagnosed as fibrous by histology, but were identified as lipid pool by IB-IVUS, which reduced its sensitivity for diagnosing fibrous lesions. The sites in which IB-IVUS indicated that fibrosis was diffusely intermingled with lipid

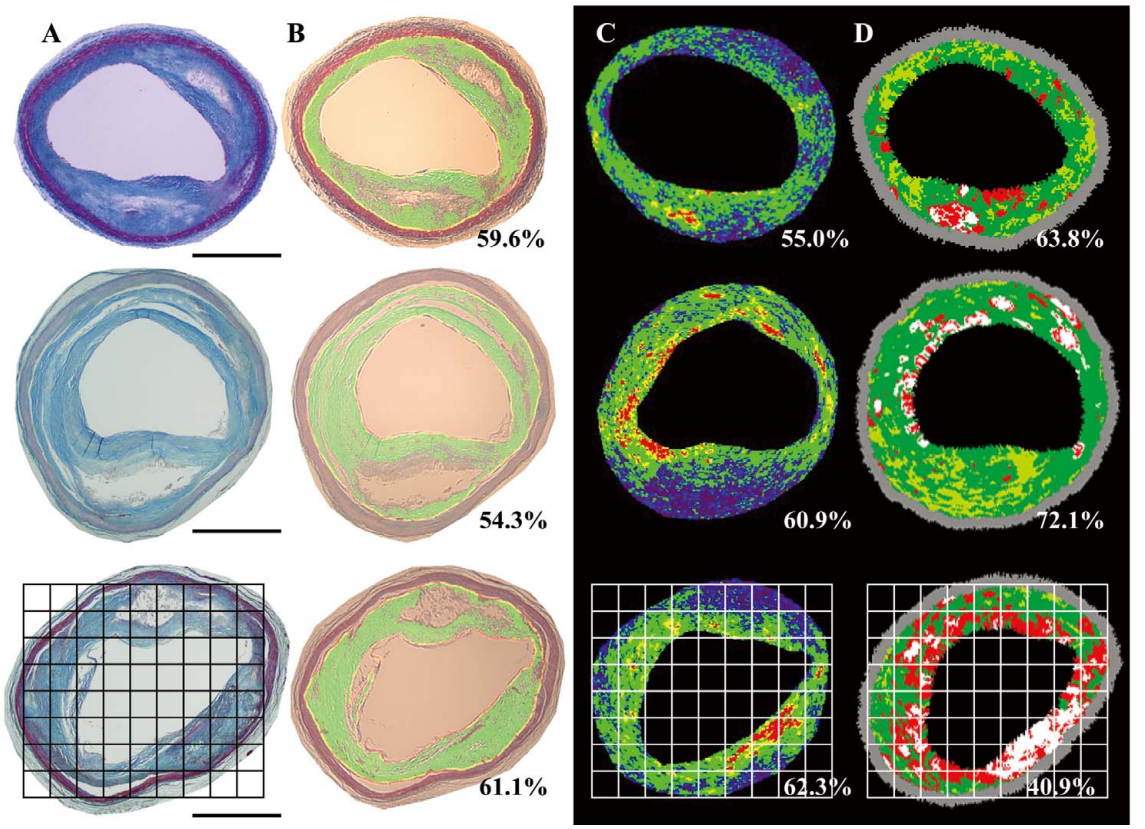

Fig 4. Representative lesion used in the direct comparison study. (A) Histological images stained with Masson's trichrome. Bar = 1 mm. (B) Images after quantification by the image processor. Areas stained blue by Masson's trichrome staining were automatically selected (green area) by the multipurpose image processor (LUZEX F) and the relative fibrous area (fibrous area/plaque area) was automatically calculated by the system. (C) Integrated backscatter-intravascular ultrasound (IVUS) images corresponding to sections analyzed by histology. (D) IVUS-Virtual Histology images corresponding to sections analyzed by histology. Percentages indicate the relative fibrous areas determined by each method. A "direct qualitative" comparison was performed by setting small (0.3×0.3 mm) regions-of-interest on the same sites in both the histological and IVUS images (Lower).

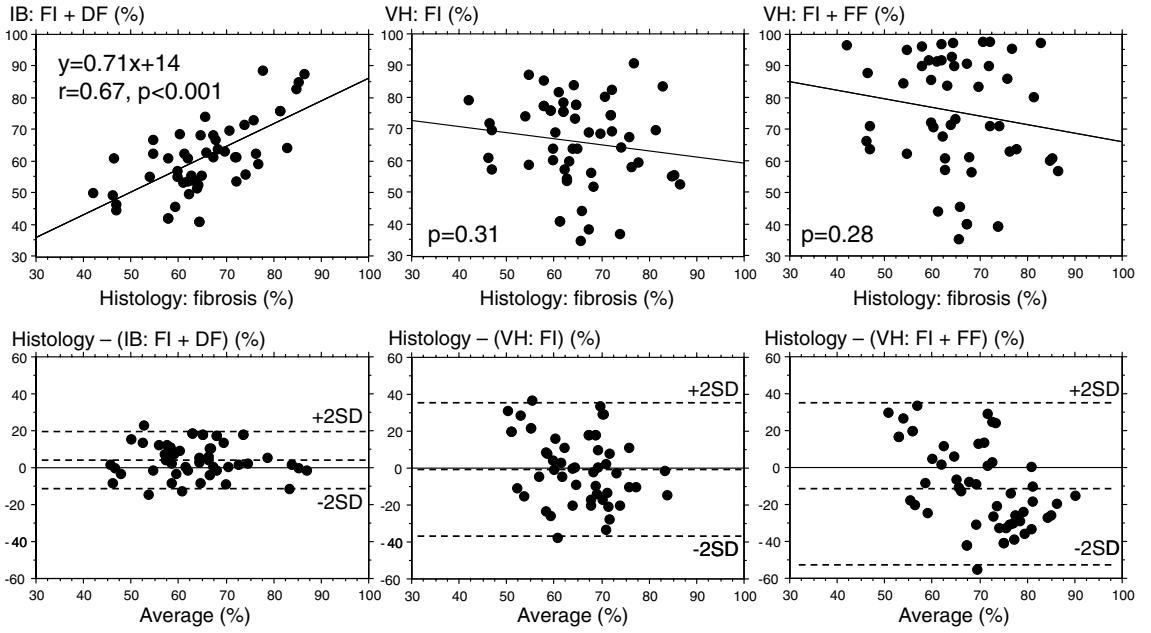

Fig 5. (Upper) Correlation between the relative fibrosis area based on histology and the % fibrosis area determined by each intravascular ultrasound system. (Lower) Bland-Altman plot. IB, integrated backscatter; VH, Virtual Histology; FI, fibrosis; DF, dense fibrosis; FF, fibrofatty.

pool were diagnosed as lipid pool by histology. These subtle differences decreased the diagnostic accuracy of IB-IVUS.

It is reported that inflammatory cells occur in 46% of fibrous caps and in 32% of the shoulder of fibrous caps.[26] In the present study, the IB values of fibrosis, which is abundant in inflammatory cells and fibroblasts, tended to be similar to the IB values of lipid pool. Therefore, a false-negative diagnosis for fibrosis was made using the IB-IVUS images. In addition, very dense fibrous lesions may produce sufficient reflectivity and attenuation or acoustic shadowing to be misclassified as calcified.[27]

In the present study, IB-IVUS occasionally underestimated calcified lesions and overestimated lipid pool behind calcification because of the acoustic shadow derived from calcification. Acoustic shadow caused by calcification hindered precise determination of the tissue characteristics of coronary plaque; however, there were many cases in which lesions that were classified as lipid pool by IB-IVUS because of the acoustic shadow behind calcification actually included a lipid core as analyzed by histology (n=16/21, 76%). Our result was concordant with previous results demonstrating that necrotic core and fibrofatty components are located behind calcification (83–89%).[28] Because calcification usually originates in lesions with lipid accumulation, the diagnosis of lipid pool by IB-IVUS in lesions behind calcification was usually accurate.

Discrepancy Between IVUS-VH Findings and Histology

In the present study, IVUS-VH overestimated the presence of necrotic core, which was located particularly close to the vessel lumen. This may have resulted in an overestimation of thin-cap fibroatheroma, as defined in a previous report[29] (Fig 3). The lesions diagnosed as lipid pool by IB-IVUS tended to show a marbled pattern in IVUS-VH, in which fibro-fatty (light-green) was intermingled with fibrous (green) (Fig 4). This may have resulted in an underestimation of fibro-fatty lesions, so that type Va lesions were misdiagnosed as type Vc lesions by IVUS-VH. A recent in vivo study using a porcine model reported that IVUS-VH was not accurate in detecting the area of each specific component within the corresponding histological specimen.[30] In the present study, neither the sensitivity nor the specificity of IVUS-VH in detecting different tissue types was as robust as validated in previous ex vivo studies. In our direct qualitative comparison, the overall agreement between the histological and IVUS-VH diagnoses was not as high (κ=0.30) as in the quantitative comparison (κ=0.73). Particularly, misdiagnoses of necrotic core and fibrosis were remarkable with regard to the precise location of each tissue component. Our results in the direct comparison study showed a tendency for the % fibrosis determined by IVUS-VH to decrease with an increase in the relative area of fibrosis based on histology. This tendency is consistent with previously-reported results.[30] In contrast, good in-vivo diagnostic accuracy of IVUS-VH compared with histology has been reported, using tissue samples obtained by directional coronary atherectomy (DCA).[24] The reason for the discrepancy in diagnostic accuracy for tissue characterization may be explained as follows. In the previous study, the comparison between IVUS-VH and histology was performed using only 1 part of the coronary specimen, whereas we compared the entire cross-section. Another reason might be that comparing tissue samples obtained by DCA is complicated, because it is hard to find the corresponding cross-section in the longitudinally compressed specimen extracted from a nose cone. However, the present study does not demonstrate that IVUS-VH is not useful for tissue characterization of coronary plaque.

Study Limitations

There were a few limitations of the ultrasound method. First, the angle dependence of the ultrasound signal makes tissue characterization unstable when lesions are not perpendicular to the axis. Picano et al reported that angular scattering behavior is large in calcified and fibrous tissues, whereas it is slight to nonexistent in normal and fatty plaques.[31] According to this report, although there was no crossover of the IB values between fibrous and fibrofatty within an angle span of 10°, or between fibrous and fatty within an angle span of 14°, this angle-dependency of the ultrasound signal might be partially responsible for the variation of IB values obtained for each tissue component. There is a report[32] that demonstrated the degree of angle-dependence of 30-MHz ultrasound in detail: the angle-dependence in the arterial intima and media was 1.11 dB/10°. Because we used a 40-MHz catheter, the angle dependence in the arterial tissue would be increased and may decrease the diagnostic accuracy for differentiating the tissue components.

Second, calcification is a perfect reflector of ultrasound, causing the acoustic shadowing so typical in IVUS images. The ultrasound signals cannot penetrate, or pass through, the calcified layer and are reflected back towards the transducer.[27] Therefore, accurate tissue characterization of the areas behind calcification is not possible, as with conventional IVUS. Likewise, IB-IVUS can not diagnose the tissue behind stents, because they are nearly perfect reflectors, causing acoustic shadowing of the ultrasound signal. This may also decrease the diagnostic accuracy for differentiating the tissue components. Third, a guidewire was not used in the process of imaging because the present studies were performed ex vivo. Imaging artifacts in vivo because of the guidewire may decrease the diagnostic accuracy. However, removal of the guidewire during imaging after completing the intervention procedure and/or excluding the area behind calcification from the analysis may be necessary in the clinical setting to eliminate this problem. Finally, detecting thrombus from a single IVUS cross-section was not possible because it is usual to look at multiple IVUS images over time for speckling, scintillation, motion and blood flow in the "microchannel".[27] The analysis of IB values in multiple cross-sections over time is required for the detection of thrombus.

Conclusions

We compared the diagnostic accuracy of IB-IVUS with IVUS-VH for tissue characterization of coronary arterial plaque using the same cross-sections and based on histology as the gold standard, IB-IVUS had higher diagnostic accuracy than IVUS-VH.

Acknowledgment

This study was supported, in part, by a research grant 18659237 (2006) from the Ministry of Education, Culture, Sports, Science and Technology of Japan.

References

1. Mizuno K, Satomura K, Miyamoto A, Arakawa K, Shibuya T, Arai T, et al. Angioscopic evaluation of coronary artery thrombi in acute coronary syndromes. *N Engl J Med* 1992; **326:** 287–291.

2. Horie T, Sekiguchi M, Hirosawa K. Coronary thrombosis in pathogenesis of acute myocardial infarction: Histopathological study of coronary arteries in 108 necropsied cases using serial section. *Br Heart J* 1978; **40:** 153–161.
3. Nissen SE, Yock P. Intravascular ultrasound: Novel pathophysiological insight and current clinical applications. *Circulation* 2001; **103:** 604–616.
4. Komiyama N, Berry GJ, Kolz ML, Oshima A, Metz JA, Preuss P, et al. Tissue characterization of atherosclerotic plaques by intravascular ultrasound radio frequency signal analyses: An in vitro study of human coronary arteries. *Am Heart J* 2000; **140:** 565–574.
5. Murashige A, Hiro T, Fujii T, Imoto K, Murata T, Fukumoto Y, et al. Detection of lipid-laden atherosclerotic plaque by wavelet analysis of radiofrequency intravascular ultrasound signals: In vitro validation and preliminary in vivo application *J Am Coll Cardiol* 2005; **45:** 1954–1960.
6. Schaar JA, De Korte CL, Mastik F, Strijder C, Pasterkamp G, Boersma E, et al. Characterizing vulnerable plaque features with intravascular elastography. *Circulation* 2003; **108:** 2636–2641.
7. Kawasaki M, Takatsu H, Noda T, Sano K, Ito Y, Hayakawa K, et al. In vivo quantitative tissue characterization of human coronary arterial plaques by use of integrated backscatter intravascular ultrasound and comparison with angioscopic findings. *Circulation* 2002; **105:** 2487–2492.
8. Kawasaki M, Sano K, Okubo M, Yokoyama H, Ito Y, Murata I, et al. Volumetric quantitative analysis of tissue characteristics of coronary plaques after statin therapy using three dimensional integrated backscatter intravascular ultrasound. *J Am Coll Cardiol* 2005; **45:** 1946–1953.
9. Sano K, Kawasaki M, Okubo M, Yokoyama H, Ito Y, Murata I, et al. In vivo quantitative tissue characterization of angiographically normal coronary lesions and the relation with risk factors: A study using integrated backscatter intravascular ultrasound. *Circ J* 2005; **69:** 543–549.
10. Nair A, Kuban BD, Tuzcu EM, Schoenhagen P, Nissen SE, Vince DG. Coronary plaque classification with intravascular ultrasound radiofrequency data analysis. *Circulation* 2002; **106:** 2200–2206.
11. Higashikuni Y, Tanabe K, Yamamoto H, Aoki J, Nakazawa G, Onuma Y, et al. Relationship between coronary artery remodeling and plaque composition in culprit lesions: An intravascular ultrasound radiofrequency analysis. *Circ J* 2007; **71:** 654–660.
12. Okubo M, Kawasaki M, Ishihara Y, Takeyama U, Kubota T, Yamaki T, et al. Development of integrated backscatter intravascular ultrasound for tissue characterization of coronary plaques. *Ultrasound Med Biol* 2008; **34:** 655–663.
13. Kawasaki M, Takatsu H, Noda T, Ito Y, Kunishima A, Arai M, et al. Non-invasive tissue characterization of human atherosclerotic lesions in carotid and femoral arteries by ultrasound integrated backscatter: Comparison between histology and integrated backscatter images before and after death. *J Am Coll Cardiol* 2001; **38:** 486–492.
14. Picano E, Landini L, Distante A, Sarnelli R, Benassi A, L'Abbate A. Different degreed of atherosclerosis detected by backscattered ultrasound: An in vitro study on fixed human aortic walls. *J Clin Ultrasound* 1983; **11:** 375–379.
15. Park JC, Siegel RJ, Demer LL. Effect of calcification and formalin fixation on in vitro distensibility of human femoral arteries. *Am Heart J* 1993; **125:** 344–349.
16. Prati F, Arbustini E, Labellarte A, Dal Bello B, Sommariva L, Mallus MT, et al. Correlation between high frequency intravascular ultrasound and histomorphology in human coronary arteries. *Heart* 2001; **85:** 567–570.
17. Stary HC, Chandler AB, Dinsmore RE, Fuster V, Glagov S, Insull W Jr, et al. A definition of advanced types of atherosclerotic lesions and a histological classification of atherosclerosis: A report from the Committee on Vascular Lesions of the Council on Atherosclerosis, American Heart Association. *Circulation* 1995; **92:** 1355–1374.
18. Virmani R, Kolodgie FD, Burke AP, Farb A, Schwartz SM. Lessons from sudden coronary death: A comprehensive morphological classification scheme for atherosclerotic lesions. *Arterioscler Thromb Vasc Biol* 2000; **16:** 1262–1275.
19. Nasu K, Tsuchikane E, Katoh O, Vince DG, Virmani R, Sumely JF, et al. Accuracy of in vivo coronary plaque morphology assessment: A validation study of in vivo virtual histology compared with in vitro histopathology. *J Am Coll Cardiol* 2006; **47:** 2405–2412.
20. Rodriguez-Granillo GA, Vaina S, Garcia-Garcia HM, Valgimigli M, Duckers E, van Geuns RJ, et al. Reproducibility of intravascular ultrasound radiofrequency data analysis: Implications for the design of longitudinal studies. *Int J Cardiovasc Imaging* 2006; **22:** 621–631.
21. Cohen J. A Coefficient of Agreement for Nominal Scales. *Educ Psychol Measurement* 1960; **20:** 37–46.
22. Fleiss JL. Statistical methods for rates and proportions, 2nd edn. New York: John Wiley & Son; 1981.
23. Kume T, Akasaka T, Kawamoto T, Watanabe N, Toyota E, Neishi Y, et al. Assessment of coronary intima–media thickness by optical coherence tomography. *Circ J* 2005; **69:** 903–907.
24. Yabushita H, Bouma BE, Houser SL, Aretz HT, Jang IK, Schlendorf KH, et al. Characterization of human atherosclerosis by optical coherence tomography. *Circulation* 2002; **106:** 1640–1645.
25. Jang IK, Tearney GJ, MacNeill B, Takano M, Moselewski F, Iftima N, et al. In vivo characterization of coronary atherosclerotic plaque by use of optical coherence tomography. *Circulation* 2005; **111:** 1551–1555.
26. Pasterkamp G, Schoneveld AH, van der Wal AC, Haudenschld CC, Clarijs RJ, Becker AE, et al. Relation of arterial geometry to luminal narrowing and histologic markers for plaque vulnerability: The remodeling paradox. *J Am Coll Cardiol* 1998; **32:** 655–662.
27. Mintz GS, Nissen SE, Anderson WD, Bailey SR, Erbel R, Fitzgerald PJ, et al. American College of Cardiology clinical expert consensus document on standards for acquisition, measurement and reporting of intravascular ultrasound studies (IVUS): A report of the American College of Cardiology task force on clinical expert consensus documents developed in collaboration with the European society of cardiology endorsed by the society of cardiac angiography and interventions. *J Am Coll Cardiol* 2001; **37:** 1478–1492.
28. Kume T, Okura H, Kawamoto T, Akasaka T, Toyota E, Neishi Y, et al. Assessment of the histological characteristics of coronary arterial plaque with severe calcification *Circ J* 2007; **71:** 643–647.
29. Rodriguez-Granillo GA, Garcia-Garcia HM, Mc Fadden EP, Valgimigli M, Aoki J, de Feyter P, et al. In vivo intravascular ultrasound-derived thin-cap fibroatheroma detection using ultrasound radiofrequency data analysis. *J Am Coll Cardiol* 2005; **46:** 2038–2042.
30. Granada JF, Wallace-Bradley D, Win HK, Alviar CL, Builes A, Lev EL, et al. In vivo plaque characterization using intravascular ultrasound-Virtual Histology in a porcine model of complex coronary lesions. *Arterioscler Thromb Vasc Biol* 2007; **27:** 387–393.
31. Picano E, Landini L, Distante A, Salvadori M, Lattanzi F, Masini M, et al. Angle dependence of ultrasonic backscatter in arterial tissues: A study in vitro. *Circulation* 1985; **72:** 572–576.
32. Courtney BK, Robertson AL, Maehara A, Luna J, Kitamura K, Morino Y, et al. Effect of transducer position on backscattered intensity in coronary arteries. *Ultrasound Med Biol* 2002; **28:** 81–91.